



Novel strategies to reduce the springback for double-sided incremental forming

Hongyan Wang¹ · Runfeng Zhang¹ · Huan Zhang¹ · Qi Hu¹ · Jun Chen¹

Received: 7 August 2017 / Accepted: 17 January 2018 / Published online: 3 February 2018
© Springer-Verlag London Ltd., part of Springer Nature 2018

Abstract

Springback is one of the key defects which influences the geometric accuracy of the incremental sheet forming parts, and it can only be controlled or compensated by optimized toolpath or tool positioning especially in double side incremental forming (DSIF). In the present work, novel strategies including ‘squeezing’ and ‘reverse bending’ are investigated targeting to reduce the springback in DSIF. Experiments and numerical simulations have been conducted to validate the effect of the new strategies. The springback has been significantly reduced with optimum process parameters.

Keywords Double-sided incremental forming · Springback · Reverse bending · Squeezing

1 Introduction

Compared with single point incremental forming (SPIF), double-sided incremental forming (DSIF) has more advantages in fabricating the sheet metal components with complicated features [1]. Although variant processes have been developed to increase its flexibility and deal with the issue of formability and geometric accuracy of incremental sheet forming (ISF), the springback after unclamping and trimming occurs unavoidably and needs to be fixed. Duflou et al. [2] adopted two different toolpath strategies (double-pass forming with pre-shaping, reverse finishing) to improve the part accuracy in SPIF. And Duflou et al. [3, 4] also deployed dynamic laser-assisted heating on the radiation of the tool contact area to fabricate cone-shaped component by SPIF, and found the residual stress level and springback were reduced. Bambach et al. [5] combined multi-stage forming and stress-relief annealing before trimming in SPIF to reduce the springback. Allwood et al. [6] demonstrated a closed-loop control strategy that allows compensation for model error in SPIF. For DSIF, Wang et al. [7] designed a C-frame with a preset gap to make the sheet metal be squeezed so

that better geometric configuration can be achieved compared with SPIF. Malhotra et al. [8] proposed that ‘squeezing toolpath’ could improve the uniform thickness distribution, and also proposed a novel accumulative double-sided incremental forming (ADSIF) strategy with the tools under displacement control along the in-to-out toolpath, and the effectiveness was proved [9]. Lingam et al. [10] designed a feature recognition methodology and automatic sequencing of features for DSIF, and achieved good accuracy for the complex freeform geometries.

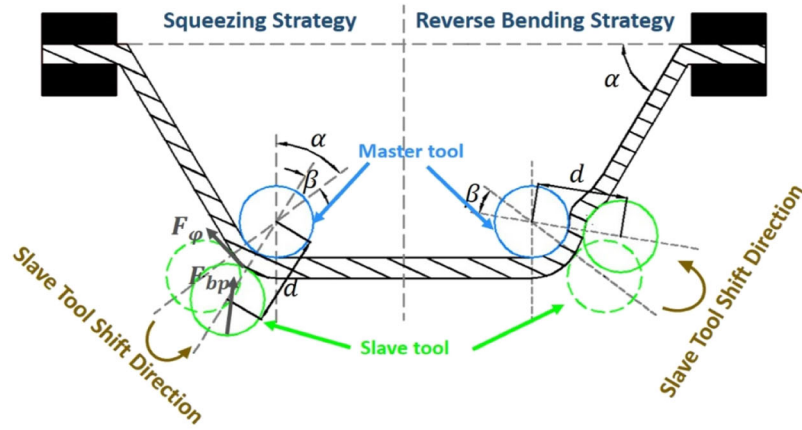
However, except the methods for SPIF, the available ideas for DSIF, unfortunately, need additional processing, which means longer processing duration. In the present work, two novel strategies are proposed for DSIF in which the two independently controlled tools cooperate with each other to generate the ‘squeezing effect’ and ‘over bending effect’ on the contact area between the tool and sheet metal. In order to validate the capabilities of the new strategies to DSIF in springback control, experiments and numerical simulations are conducted on a specific component with an ellipsoid feature. The profile and springback are analyzed after unclamping and trimming operations.

✉ Jun Chen
jun_chen@sjtu.edu.cn

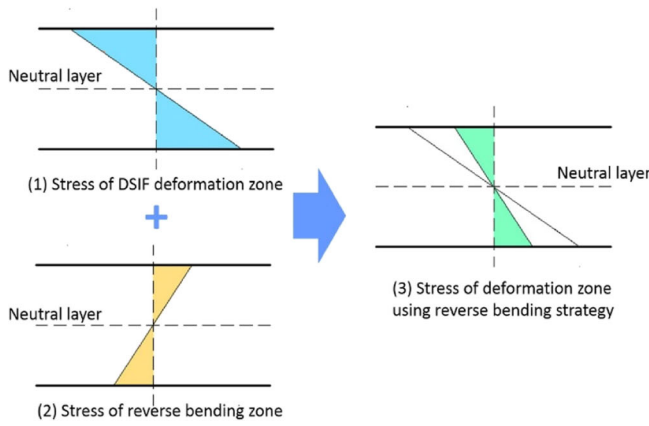
¹ Department of Plasticity Technology, Shanghai Jiao Tong University, Shanghai 200030, China

2 Strategies

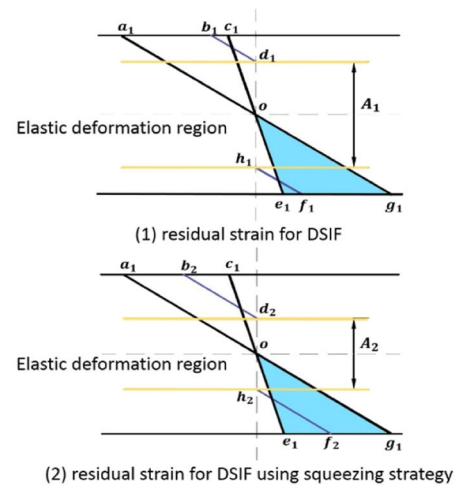
To reduce the springback of DSIF, there are two strategies to be investigated as shown in Fig. 1.



(a) illustration of the two strategy

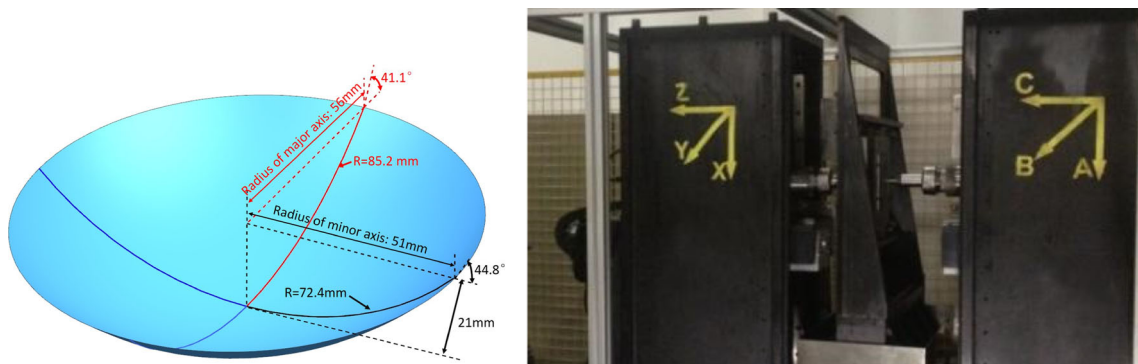


(b) Residual stress under reverse bending strategy



(c) Residual stress under squeezing strategy

Fig. 1 Illustration of the two strategies to reduce springback of DSIF. a Illustration of the two strategy. b Residual stress under reverse bending strategy. c Residual stress under squeezing strategy



(a) The designed part

(b) The DSIF prototype

Fig. 2 Experiment setup. a The designed part. b The DSIF prototype

Table 1 Experiment plan

| Experiment number | Forming type | Rotation angle β | Back pressure | Distance between the centers of the two tools |
|-------------------|---------------------------|------------------------|---------------|---|
| 1 | Normal DISF | W/ tool shift | 0 | $2 * R + t * \cos \alpha$ |
| 2 | DISF with reserve bending | 8° | 0 | $2 * R + t * \cos \alpha$ |
| 3 | | 16° | 0 | $2 * R + t * \cos \alpha$ |
| 4 | | 24° | 0 | $2 * R + t * \cos \alpha$ |
| 5 | | 32° | 0 | $2 * R + t * \cos \alpha$ |
| 6 | DISF with squeezing | w/ tool shift | 360 N | $2 * R + t * \cos \alpha$ |
| 7 | | w/ tool shift 50% | 360 N | $2 * R + t * \cos \alpha$ |
| 8 | | w/ tool shift 100% | 360 N | $2 * R + t * \cos \alpha$ |

2.1 Reverse-bending

The reverse-bending strategy shown on the right side of Fig. 1a is inspired by roller leveling process (RLP). During RLP, the alternating bending could produce flat and nearly stress-free sheet metals. Based on this idea, during DSIF, the sheet metal deforms under the pressure from the master tool, while the slave tool generates a reverse bending at the already-deformed region.

The schematic on how the reverse bending uniforms the stress distribution is shown in Fig. 1b. When the master tool passes a specific region, the stress distribution will be generated as shown in Fig. 1b (1). As the deformed sheet metal is still clamped, the stress cannot be fully released. If the slave tool is designed to pass the same region, it will generate a reverse bending and the generated stress is shown in Fig. 1b (2). By superimposing these two stress fields together, the amount of the stress can be reduced as shown in Fig. 1b (3).

Table 2 Simulation models and parameters

| Attribute | Comment |
|---|--|
| Hardening rule (isotropic hardening) | $\sigma_y = k \varepsilon^n = k (\varepsilon_{yp} + \bar{\varepsilon}^p)^n$, $k = 437, n = 0.21$ |
| Yield function model | von Mises yield criterion |
| Yield stress (MPa) | 384.3 |
| Poisson ratio | 0.33 |
| Element type | Full integrated shell |
| Number of integration points | 5 through the thickness |
| Scaled tool velocity | 1000 mm/s |
| Friction coefficient between the tool and the sheet metal | 0.02 |

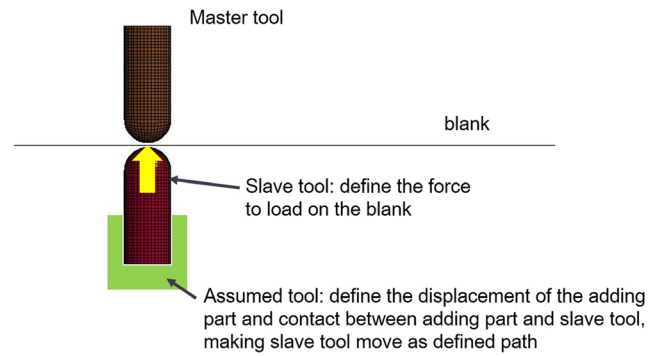


Fig. 3 Numerical simulation model for boundary condition of DSIF

2.2 Squeezing

During DSIF, with the sheet metal squeezed by the two tools, it is possible to change the stress distribution in the deforming zone. Lu et al. [11] proved that the formability under DSIF can be improved with increased hydrostatic pressure. Different tool shifts will be studied to minimize the springback.

As shown in the left side of Fig. 1a, the component of back pressure along the contacting line F_φ weakens the tensile

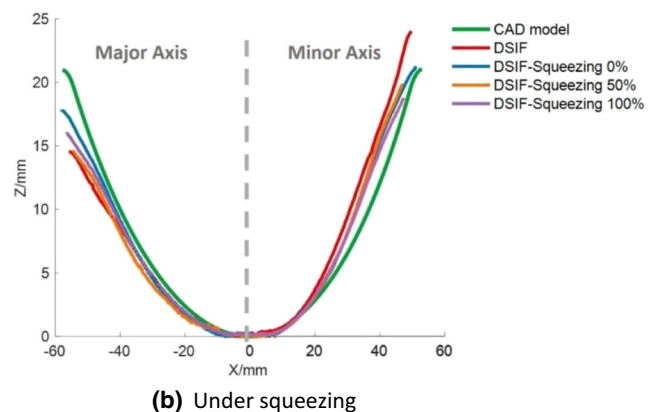
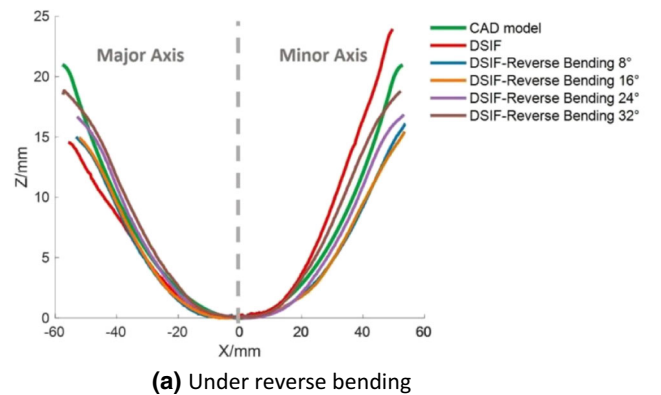


Fig. 4 Sectional profiles after trimming. **a** Under reverse bending. **b** Under squeezing

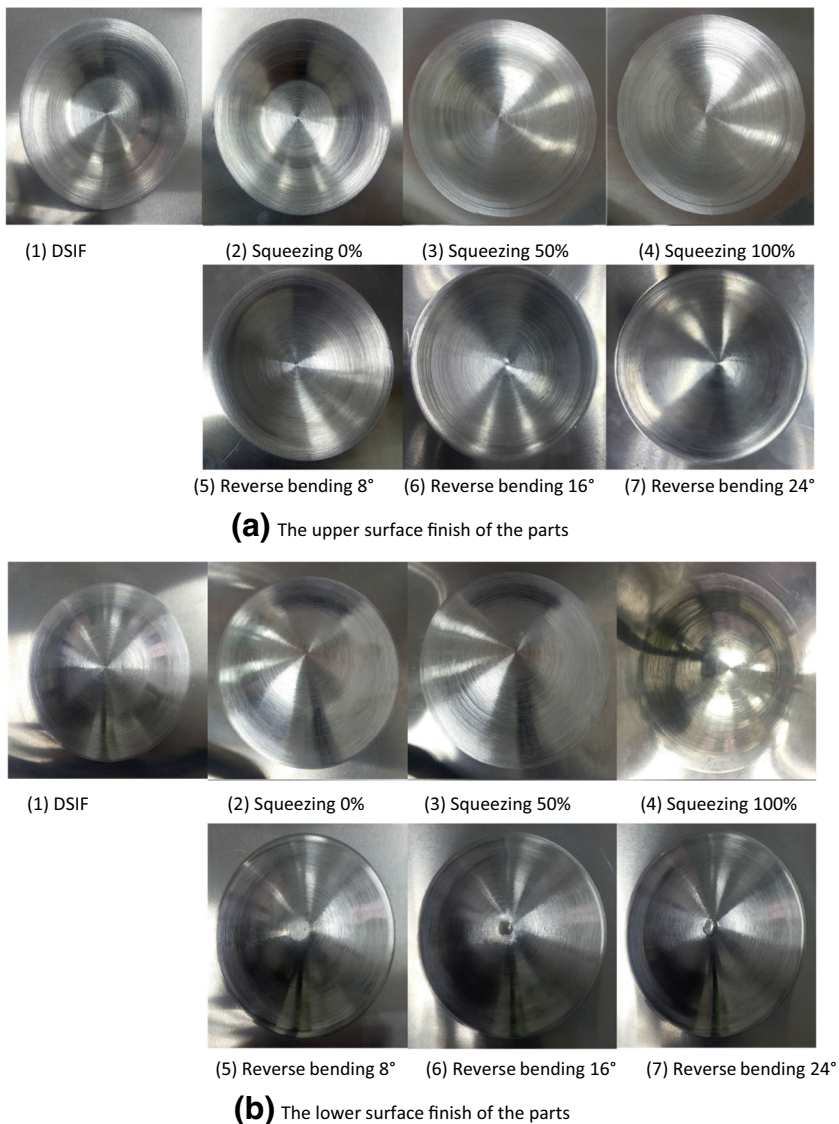
stress of the deformation zone, which makes the elastic deformation region decrease. Figure 1c illustrates the residual strain distribution along the thickness of the deformed material. In the schematic, A_1 、 A_2 represent elastic deformation region through the blank. $(a_1 - o - g_1)$ represents strain before external force releases, while $(c_1 - o - e_1)$ means theoretical strain after external force releases, and $(b_1 - d_1 - o - h_1 - f_1)$, $(b_2 - d_2 - o - h_2 - f_2)$ represent final strain after external force releases. The decreased elastic deformation region $A_1 < A_2$, leading to $b_1 < b_2$, means that the actual elastic strain variation is much less so that the springback can be dramatically reduced.

3 Experiment

A cone part with ellipsoid section (major axis 56 mm; minor axis 51 mm; depth 21 mm) is designed to validate the pro-

posed method shown as Fig. 2a. The sheet metal is AA7075 with initial thickness as of 1 mm. The two strategies for DSIF process has been implemented by an in-house prototype system shown as Fig. 2b, on which the two synchronous tools can move along the predefined tool trajectories. The diameters of both tools are 10 mm, and the feed rate for each tool is 1200 mm/min. An air cylinder is employed to support the slave tool so as to generate the designed back pressure. The spiral tool path with a constant scallop height of 0.02 mm is employed. To reduce the friction between the tool and the sheet metal, Rocol RTD paste is employed as the lubricant. After the forming process, a KEYENCE® LK-G150 laser displacement sensor is employed to measure the cross-sectional configuration. Compared with conventional truncated cone or pyramid shape, the ellipsoid shape has special springback characteristics in major axis section and minor axis section. The experiment plan is listed in Table 1.

Fig. 5 The formed parts of different cases. (1) DSIF. (2) Squeezing 0%. (3) Squeezing 50%. (4) Squeezing 100%. (5) Reverse bending 8°. (6) Reverse bending 16°. (7) Reverse bending 24°. **a** The upper surface finish of the parts. **b** The lower surface finish of the parts



4 Numerical simulation

Numerical simulations have also been conducted using LS-Dyna to track the springback evolution during the forming, unclamping, and trimming processes, and to investigate the springback under different forming conditions. The trimming shape and dimension is the same as experiment as shown in Fig. 2a. The simulation models and parameters are listed in Table 2.

Since the displacement boundary and the force boundary cannot be defined simultaneously, an assumed tool is employed to define the displacement of the slave tool, and the back pressure is defined on the slave tool. The model is shown in Fig. 3.

5 Results and discussions

5.1 Experimental results and discussion

Reverse-bending and squeezing were applied to DSIF, and the sectional profiles are measured and shown in Fig. 4. It shows that the springback in major-axis section goes outwards and inwards in minor-axis section for traditional DSIF. The proposed strategies do not change the mode of springback, but reduce the amount of springback.

Under reverse bending, Fig. 4a shows that if the reverse bending angle is set as 24° , the part sectional profiles meet the CAD model most in both major axis and minor axis. Under squeezing, Fig. 4b shows that by changing the position of slave tools, the final geometric variation varies. If the slave tool is at the position of 100% offset, which means the percentage of deviation angle ($\text{per} = \beta/\alpha$) is 100%, the final deviation is smaller than that at 0% offset or 50% offset. As can be seen, the best performance of squeezing strategy is not as effective as the best performance of reverse bending strategy.

The formed parts by DSIF with squeezing or with reverse bending are shown in Fig. 5. Both master tool and slave tool follow the specified tool paths with very small constant scallop height as 0.02 mm so that the sheet metal can deform sequentially and incrementally with very small step, and this is the reason why the surface finish of each side of the parts made by DSIF with squeezing or with reverse bending does not show any differences compared with that made by traditional DSIF.

5.2 Numerical simulation results and discussion

Numerical simulation results are shown in Fig. 6, which reveals that both reverse bending and squeezing can reduce the springback. And similar to the experimental

results, predicted springback of the major axis is more obvious than of minor axis. The springback in all cases under reverse bending is within 0.5 mm, while within 0~1.6 mm under squeezing, this means reverse bending is more effective than squeezing. Comparisons of the effect of different strategies show that the springback is the minimum under reverse bending with the angle as 24° , while the springback is the least under squeezing with the tool shift as 100%. These results correspond to the experiments.

The springback distributions after each process under different strategies are shown in Fig. 7. It is found that the springback amount is still temporarily suppressed even after unclamping, the springback amounts in all cases under reverse bending are within $-0.25\sim 0.25$ mm, while within $-0.4\sim 0$ mm under squeezing. After trimming, the springback is further released, and is within $-0.5\sim 0.5$ mm under reverse bending while $-1.2\sim 1.4$ mm under squeezing. Similar with experimental results, the simulation results also demonstrate that reverse bending is more effective than squeezing in minimizing the springback amount and the deviation, and DSIF under reverse bending with bending angle as 24° results in the smallest springback among all the designated plan.

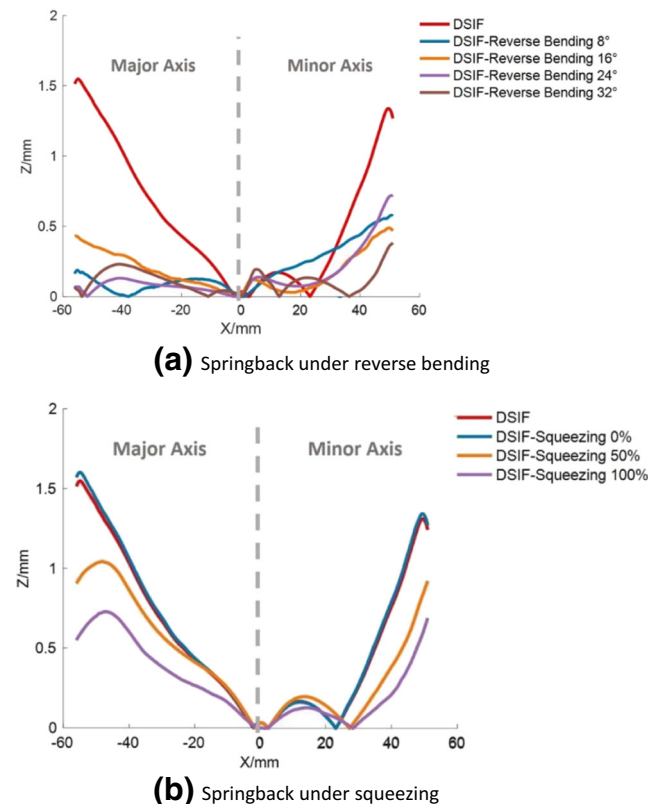


Fig. 6 Springback of different cases. **a** Springback under reverse bending. **b** Springback under squeezing

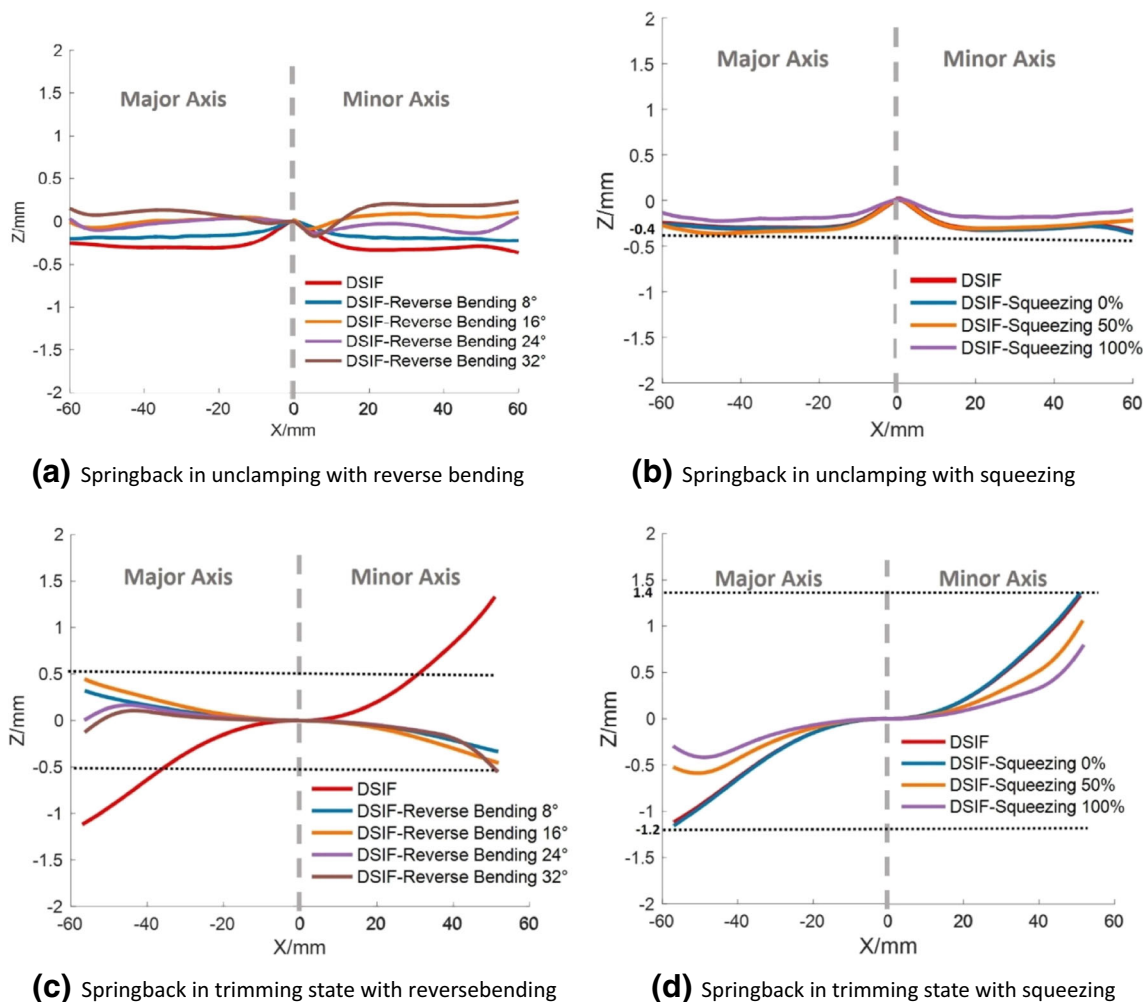


Fig. 7 Springback in different states. **a** Springback in unclamping with reverse bending. **b** Springback in unclamping with squeezing. **c** Springback in trimming state with reverse bending. **d** Springback in trimming state with squeezing.

6 Conclusions

In the present work, two strategies—reverse bending and squeezing have been proposed to integrate with DSIF and experimentally investigated with different process parameters to reveal their effects on reducing the final springback of the DSIF part, and numerical simulations have also been conducted to track the history of springback evolution during unclamping and trimming. The simulation results meet well with experiments, and the main conclusions are summarized as follows.

Both reverse bending and squeezing can decrease the springback of DSIF part, and reverse bending looks more effective to reduce the amount of the springback.

Under reverse bending, the springback decreases with the increasing reverse bending angle. The smallest springback can be achieved with the reverse bending angle set at 24°.

Simulation results reveal that trimming results in more severe springback than unclamping.

Acknowledgements The authors are grateful for the financial support from National Natural Science Foundation of China through grant #51675332.

References

- Zhang RF, Lu B, Chen J (2016) Development of a multi-pass double side incremental forming strategy for forming complex sheet metal parts with a step feature. *J Shanghai Jiao Tong Univ* 50(9): 1333–1338 (in Chinese)
- Duflou JR, Lauwers B, Verbert J (2007) Study on the achievable accuracy in single point incremental forming. *Adv Met MaterForm*: 251–262
- Duflou JR, Callebaut B, Verbert J, De Baerdemaeker H (2007) Laser assisted incremental forming: formability and accuracy improvement. *CIRP Ann Manuf Technol* 56(1):273–276. <https://doi.org/10.1016/j.cirp.2007.05.063>
- Duflou JR, Callebaut B, Verbert J, De Baerdemaeker H (2008) Improved SPIF performance through dynamic local heating. *Int J Mach Tools Manuf* 48(5):543–549. <https://doi.org/10.1016/j.ijmachtools.2007.08.010>

5. Bambach M, Taleb Araghi B, Hirt G (2009) Strategies to improve the geometric accuracy in asymmetric single point incremental forming. *Prod Eng* 3(2):145–156
6. Allwood JM, Music O, Raithathna A, Duncan SR (2009) Closed-loop feedback control of product properties in flexible metal forming processes with mobile tools. *CIRP Ann Manuf Technol* 58(1):287–290. <https://doi.org/10.1016/j.cirp.2009.03.065>
7. Wang Y, Huang Y, Cao J, Reddy NV (2008) Experimental study on a new method of double side incremental forming. *International manufacturing science and engineering conference collocated with the 3rd JSME/ASME international conference on materials and processing*, pp. 601–607
8. Malhotra R, Cao J, Ren F, Kiridena V, Xia ZC, Reddy NV (2011) Improvement of geometric accuracy in incremental forming by using a squeezing toolpath strategy with two forming tools. *J Manuf Sci Eng* 133(6):061019. <https://doi.org/10.1115/1.4005179>
9. Malhotra R, Cao J, Beltran M, Xu D, Magargee J, Kiridena V, Xia ZC (2012) Accumulative-DSIF strategy for enhancing process capabilities in incremental forming. *CIRP Ann Manuf Technol* 61(1): 251–254. <https://doi.org/10.1016/j.cirp.2012.03.093>
10. Lingam R, Prakash O, Belk JH, Reddy NV (2017) Automatic feature recognition and tool path strategies for enhancing accuracy in double sided incremental forming. *Int J Adv Manuf Technol* 88(5-8):1639–1655. <https://doi.org/10.1007/s00170-016-8880-1>
11. Lu B, Fang Y, Xu DK, Chen J, Ai S, Long H, Ou H, Cao J (2015) Investigation of material deformation mechanism in double side incremental sheet forming. *Int J Mach Tools Manuf* 93:37–48. <https://doi.org/10.1016/j.ijmactools.2015.03.007>